RSC Advances

ROYAL SOCIETY OF CHEMISTRY

www.rsc.org/advances

Journal Name

RSCPublishing

ARTICLE

Photoelectrochemical Determination of Intrinsic Kinetics of Photoelectrocatalysis Processes at {001} Faceted Anatase TiO_2 Photoanode

Cite this: DOI: 10.1039/x0xx00000x

Received 00th January 2012,
Accepted 00th January 2012

DOI: 10.1039/x0xx00000x

www.rsc.org/

Tao Sun,[a] Yun Wang,[*a] Mohammad Al-Mamun,[a] Haimin Zhang,[a] Porun Liu,[a] and Huijun Zhao[*a,b]

The understanding the intrinsic degradation kinetics of organic species at the reactive anatase TiO_2 (001) surfaces under operational conditions is essential for the development of photoelectrocatalytic treatment of wastewater or polluted air. In this study, the intrinsic degradation kinetics of oxalic acid on the anatase (001) surface is successfully investigated by using a facile photoelectrochemical (PEC) method. A double-layered TiO_2 photoanode mainly exposed by anatase {001} facets is purposely designed for the PEC measurements. The results reveal that the adsorption of oxalic acid follows the Langmuir adsorption model within the investigated concentration range. The PEC degradation profile can be fitted by two different first-order kinetic processes. The measured rate constant for the fast degradation processes is five times higher than that of the slow processes. The results confirm that the anatase TiO_2 with exposed (001) surface possesses a higher reactivity than that of {101} faceted anatase TiO_2.

Introduction

Photo-degradation of organic species by semiconductors, such as titanium dioxides (TiO_2), is one of the attractive approaches for the treatment of wastewater and polluted air.[1, 2] A meaningful measurement of intrinsic kinetics of photoelectrocatalytic reactions can provide insightful information of the photocatalytic degradation process, critically important for photocatalysis applications.[3-6] However, the most of reported photoelectrocatalytic kinetics studies are focused on the apparent reaction kinetics, which are a collective result of many factors. In addition, the apparent kinetics measurement methods are inadequate for directly investigating the overall kinetics of photocatalysis because their inability to determine the instantaneous reaction rate constant. Moreover, the degradation kinetics of strong adsorbates on a highly photoactive surface is difficult because the initial rate cannot be precisely defined due to the adsorption of analytes on the electrode surface. Thus, it is difficult to establish a precise relationship between the adsorption strength of organic species and the apparent reaction rates. To this end, it becomes rather challenging to experimentally measure the adsorption properties under operational conditions. One breakthrough is the introduction of a simple, rapid and accurate photoelectrochemical (PEC) method to directly and spontaneously characterize thermodynamic and instant kinetic properties for adsorption and degradation of organic species at the surface of photocatalysts.[7-12] Another attraction of PEC measurement is that it allows the investigation of intrinsic degradation kinetics without the influence of other factors such as mass transfer and the reduction processes.[9, 13, 14] Therefore, the intrinsic reaction rates obtained from PEC measurements can be strongly correlated to the adsorption strength of adsorbates under operational conditions.

It is well know that the photoelectrocatalytic reactivity of inorganic crystals is also governed by the surface geometric structures.[15-20] Among all TiO_2 surfaces, the anatase (001) surface has been theoretically predicated to possess high reactivity.[9, 12, 21-23] However, the majority of the reported studies on photocatalytic degradation kinetics of organic species at the anatase (001) surface have been performed by the measurement of the rate of the reactant disappearance to determine the apparent rate of reaction.[20, 24-26] Although there have been some PEC studies of the oxidative degradation of organic species at different TiO_2 surfaces,[9, 11, 12, 23, 27] to our knowledge, there has no report on determination of the intrinsic degradation kinetics of organic species at the reactive anatase (001) surface.

The photocatalytic degradation of organics is essentially an interfacial electron transfer process for which the reactant adsorption at the catalyst surface plays a critical role to affect

the kinetic behaviour of the reaction system[10]. Nevertheless, the precise determination of adsorption at a catalysts surface by traditional methods is tedious, time consuming and inaccurate.[9, 27] Additionally, the adsorption of organics at the {001} faceted anatase TiO_2 surface has not yet been reported. Therefore, it would be attractive to determine the adsorption properties of {001} faceted anatase TiO_2 in a simple, rapid and effective manner.

In this study, a PEC method[8-10, 12-14, 28, 29] is employed to quantitatively investigate the surface adsorption properties and the kinetic processes of photocatalytic degradation of oxalic acid at the {001} facet dominated anatase TiO_2 photoanode by determining the adsorption constant and the instantaneous inherent rate constant.

Experimental section

Preparation of TiO_2 photoanodes

In this study, three types of photoanodes were fabricated by immobilising TiO_2 onto a FTO conductive substrate (45mm×15mm×2mm).

The dense film photoanode (denoted as DF photoanode) was fabricated using a dip-coating method. An aqueous colloidal TiO_2 was firstly prepared by hydrolysing titanium butoxide.[30] The resultant colloidal solution contains ca. 60 g/dm^3 of TiO_2 solid with particle sizes ranging from 8 to 10 nm. The carbowax (30% w/w based on the solid weight of the TiO_2 colloids) was then added to form the coating solution. The FTO glass slides were cleaned by deionized water, 2-propanol and acetone mixed solution before use as the substrate. The cleaned slides were immersed in coating solution and then withdrawn at a speed of 2 mm/s to control the TiO_2 film thickness. The coated substrates were dried in air and then calcinated at 450 ˚C for 2 hours in a muffle furnace (Fig. S1, ESI†). The thickness of the DF photoanode was measured to be 600 nm by the profilometer.

The {001} faceted single-layer anatase TiO_2 film photoanode (denoted as A001 photoanode) was fabricated using a reported method.[24] Briefly, 2.808 g NaCl was mixed with 60 ml 0.04 M TiF_4 solution, which was prepared by adding 0.297 g of TiF_4 into 60 ml of 0.01 M HCl, in a Teflon-lined stainless steel autoclave (100 ml volume). The solution was stirred at ambient conditions for 10 min to ensure a complete dissolution. FTO glasses were cleaned by washing with deionized water, 2-propanl and acetone, respectively before being immersed into the solution and placed against the Teflon-liner wall at an angle with the conducting side facing down. The autoclave was heated to 200 ˚C in an oven. The hydrothermal reaction duration has been demonstrated to greatly affect the morphology of TiO_2 crystals.[31] Four-hour hydrothermal duration was set in this study because at which the products possess the highest percentage of exposed {001} facets (Fig. S2, ESI†). The resultant coatings were then removed from the autoclave and rinsed with deionized water and dried in air at 50 ˚C for 30 minutes. The A001 photoanode was obtained by calcinating the resultant coatings in a tube furnace at 450 °C for 2 hours in air with a heating rate of 5 °C/min.

A two-step procedure was used to fabricate the double-layered photoanode with a dense bottom layer and {001} faceted anatase TiO_2 top layer (denoted as DL photoanode). The first step was to coat a dense film onto the FTO substrate with the same procedure used for fabrication of DF photoanode. The DL photoanode was fabricated using the resultant dense film coated substrate as the 'substrate' to further grow the top A001 layer with the same hydrothermal method used for fabrication of A001 photoanode.

Characterization

The obtained products were comprehensively characterized by Scanning electron microscopy (SEM, JSM-6300F), transmission electron microscopy (TEM, Philips F20), and X-ray diffraction (XRD, Shimadzu XRD-6000 diffractometer).

PEC measurements

All PEC measurements were conducted in a three-electrode PEC cell with a quartz window (0.785 cm^2) for ultraviolet (UV) illumination.[1, 14, 27, 32, 33] The TiO_2 photoanodes were used as the working electrode, and a platinum mesh and a saturated Ag/AgCl were used as the counter and reference electrodes, respectively. A 0.1 M $NaNO_3$ solution is used as the electrolyte. A voltammograph (CV-27, BAS) was employed for the application of potential bias. The photocurrent signals and potential were recorded using a Maclab 400 interface (AD Instruments). UV illumination was carried out by a 150 W Xenon arc lamp light with focusing lenses (HF-200W-95, Beijing Optical Instruments). To avoid the electrolyte being heated-up by the infrared light, a UV-band pass filter (UG 5, Avotronics Pty. Ltd.) was utilized. The UV light intensity was regulated and carefully measured at 400 nm.

Since the *ex-situ* PEC measurements can exclude the effects of mass transfer of organic species in solution, this specific method was adopted to measure the thermodynamic and kinetic properties during PEC degradation of oxalic acid at TiO_2 photoanodes. Before the PEC measurement, the photoanode was immersed in a 0.1 M $NaNO_3$ solution with given concentration of oxalic acid at pH 4.0. After the pre-adsorption of organic species reached equilibrium, the photoanode was removed from the adsorption solution, adequately rinsed by 0.1 M $NaNO_3$ solution, and immediately transferred into the PEC cell for PEC measurements under a UV light intensity of 5.0mW/cm^2.

Result and discussion

TiO_2 photoanodes with dominated {001} facets

To enable a PEC measurement, a photoanode with immobilised {001} faceted anatase TiO_2 needs to be fabricated. However, the synthesis of anatase crystals with exposed {001} facets is

challenging because of their high surface energies.[31] In 2008, TiO_2 nanocrystals with a large percentage of {001} facets have been successfully synthesized through the fluorination techniques.[15, 25, 34] Recently, the immobilization of {001} faceted TiO_2 nanoparticles has been reported.[31,35]. In this work, A001 photoanode with a single layer {001} faceted anatase TiO_2 film was fabricated using the method reported by Liu *et al*.[31] The XRD patterns shown in Fig. 1a confirm that the synthesized materials are anatase TiO_2. Fig. 1b and c are typical surface and cross-sectional field emission SEM (FESEM) images of A001 photoanode, revealing an approximately 1 µm thick randomly packed TiO_2 nanosheets.[26] Fig. S3 shows the high resolution transmission electron microscopy (HRTEM) image and selected area electron diffraction (SAED) pattern of the nanosheets, confirming that the nanosheets are formed by 89% exposed {001} facets. The linear sweep voltammograms (LSVs) of the single-layered A001 photoanode under different UV illumination intensities are shown in Fig. 1d. It was found that for all cases investigated, the measured photocurrents increased with the applied potential bias and no saturation can be attained within the applied potential range, which is unsuitable for PEC measurements. This is because the PEC methods[11, 12, 27] used in this work are based on the measurement of the photocurrent/charge originated from the oxidative degradation of oxalic acid. These measurement principles are valid only when the photocurrent profiles are measured at a potential bias where 100% of photogenerated electrons are collected, which can be determined by LSV experiments. In short, under UV illumination, a suitable PEC photoanode should possess a LSV response that initially linearly increased with the applied potential bias (because the electron transport inside the catalyst film is the rate-determining step) and then saturated at more positive potentials (because 100% of photogenerated electrons being collected).[10-12, 27] One possible reason for the non-saturation behaviour of the single-layered A001 photoanode could be due to the existence of the voids in the large anatase TiO_2 nanosheets immobilized on the FTO substrate that allow the electrolyte to directly access to the FTO substrate, leading to a back reaction of photoinjected electrons.[36] Under the circumstance, the FTO substrate act as an electrode and the measured current would increase with the increased potential bias.

In order to block the electrolyte directly access to the FTO substrate, a double-layered photoanode (DL photoanode) with a dense bottom layer and an A001 top layer was fabricated. Fig. 1e and f show typical surface and cross-sectional FESEM images of DL photoanode. TEM and HRTEM images, and SAED pattern (Fig. 1g) confirm that the top layer is formed by the {001} faceted anatase TiO_2 nanosheets.[25] The LSVs of DF photoanode with a single layer dense film under different UV illumination intensities confirm that the saturated photocurrents can be attained for all cases investigated (Fig. S4a, ESI†), which are similar to the previous report using the same type photoanode. This demonstrates that a dense film is capable of effectively block the direct electrolyte access to the FTO substrate. The LSVs of DL photoanode under different UV illumination intensities are given in Fig. 1h. The results reveal that for all cases investigated, the photocurrent responses initially increased linearly with the potential bias and saturated when the applied potential bias is more positive than +0.30 V (vs Ag/AgCl electrode). This means that for the DL photoanode, a 100% electron collection efficiency can be achieved when an applied potential bias is more positive than that of +0.30V. For better assurance, a +0.40V potential bias is selected for all subsequent experiments. Under different UV light intensities, the demonstrated linear relationship between light intensities and the saturated photocurrents at the potential bias of +0.4 V (Fig S4b, ESI†) further confirms that the DL photoanode can satisfy the requirements of the PEC measurements in this work if a +0.40 V potential bias is used.

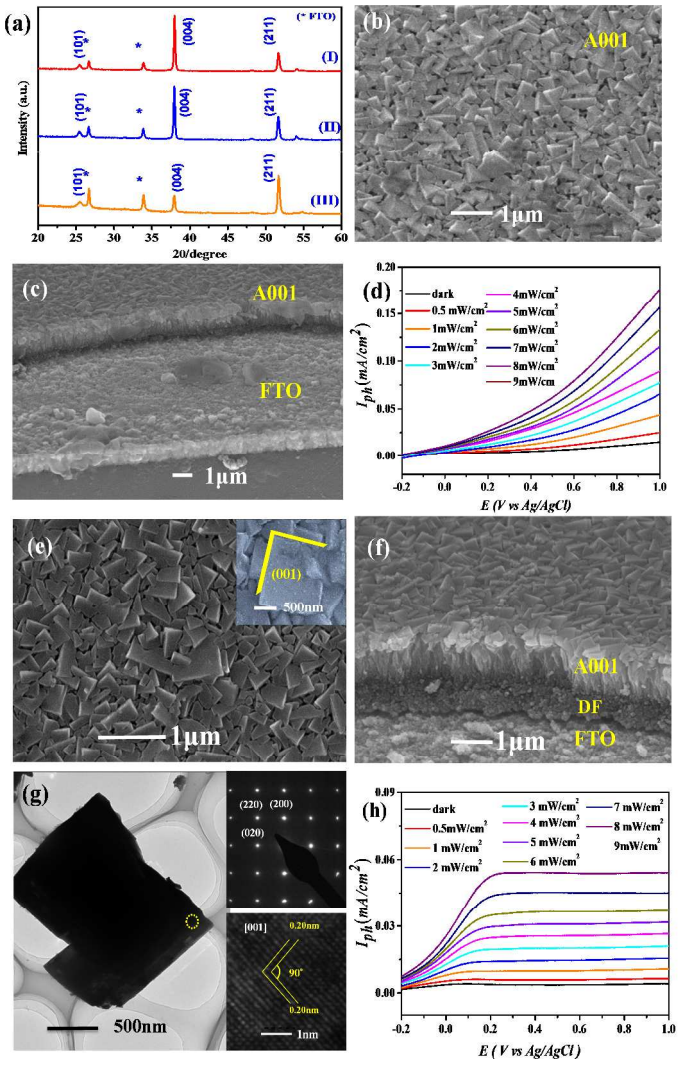

Fig. 1 (a) XRD patterns of (I) A001, (II) DL and (III) DF photoanodes (the peaks with * are from the FTO substrates); (b) and (c) Surface and cross-sectional FESEM images of A001 photoanode; (d) LSV of A001 photoanode under different UV illuminations intensities; (e) and (f) Surface and cross-sectional FESEM images of DL photoanode; (g) TEM (left), SAED (top right), and HRTEM (bottom right) images of the DL photoanode; (h) LSVs of DL photoanode under different UV illuminations intensities.

Adsorption properties

The photocatalytic degradation efficiency depends largely on the adsorption properties of organic species on the TiO_2 surface.[4, 6, 37] To validate the photoelectrocatalytic performance of the anatase TiO_2 (001) surface, an *ex-situ* measurement approach was adopted in this work to qualitatively investigate the surface adsorption properties of {001} faceted photoanode. The oxalic acid is chosen because it is one of the most studies organic species for photocatalytic degradation with great adsorption strength on TiO_2 surfaces.[9, 32, 33, 38, 39] The mineralization of one oxalic molecule required only two electrons and involves the least number of intermediates, which make its overall photocatalytic degradation process simple.

Initially, the TiO_2 photoanodes were immersed in solutions containing different concentrations of oxalic acid for pre-adsorption. The pre-adsorption time should be long enough to guarantee the pre-adsorption reaches the equilibrium. The relationship between the pre-absorption time and overall net transferred charge (Q) resulted from the mineralization of oxalic acid with a concentration of 0.2 mM was used to determine the per-adsorption time. The Q values are quantified by deducting the changes obtained from integrating photocurrents before and after pre-adsorption (the shaded area in Fig. S5, ESI†).[14, 27] Fig. S6 confirms that the Q values become steady when the pre-adsorption time exceeds 15 min, indicating equilibrium status has been achieved. For a better assurance, 20 min pre-adsorption time was used in this work. After the pre-adsorption equilibrium was reached, the photoanodes were removed from the adsorption solution and washed by the 0.1 M $NaNO_3$ solution before they were used to perform PEC measurements.

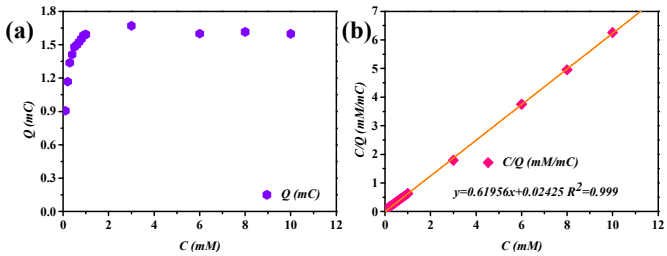

Fig. 2 (a) Plot of Q against the concentration of oxalic acid; (b) Data fitting according to the Langmuir adsorption model shown in Eq (1).

For PEC measurement, the Langmuir adsorption model can be rewritten as:[27]

$$\frac{C}{Q} = \frac{1}{Q_{max}} C + \frac{1}{Q_{max}} \frac{1}{K} \quad (1)$$

where, Q is the net charge originated from mineralisation of adsorbed organic species; C is the pre-adsorption solution concentration of organic species; Q_{max} is equivalent to the maximum surface coverage; K is the adsorption equilibrium constant, which is related to the adsorption energy of organic species on the catalysts surfaces.

According to Eq (1), a plot of C/Q against C should give a linear relationship and Q_{max} and K values can thus be determined from the slope and intercept of the plot.

Fig. 2a shows the measured $Q - C$ relationship for oxalic acid with concentrations ranged from 0.1 to 10.0 mM. The corresponding fitting plot for C/Q and C (Fig. 2b) shows a linear (R^2=0.993) relationship, confirming that the adsorption of oxalic acid on the anatase TiO_2 (001) surfaces follows the Langmuir adsorption model within the considered concentration range. The Q_{max} value obtained from Fig. 2b is 1.61 mC, which is almost identical to that by using the single layered DF electrode (Q_{max}=1.60 mC, see Fig. S7, ESI†). Since Q_{max} represents the maximum saturated adsorption coverage of adsorbents, the similar Q_{max} values indicate the surface coverage of adsorbed oxalic acid on the on the surface of {001} faceted anatase TiO_2 photoanode is close to that on the surface of the DF photoanode. However, the adsorption constant of oxalic acid (K) on the surface of {001} faceted anatase TiO_2 photoanode is $2.55 \pm 0.96 \times 10^4$ M^{-1}, which is *ca.* 30% larger than that on the surface of the DF photoanode ($K = 1.92 \pm 0.4 \times 10^4$ M^{-1}, Fig. S7, ESI†). Since the DF photoanode is dominated by the exposed {101} facets, the measured adsorption properties support that the reactivity of the anatase (001) surface is higher than that of the anatase (101) surface.[21, 22]

Intrinsic Kinetics properties

Understanding intrinsic kinetics is crucially important for catalysts design and performance improvement.[3] Theoretically, a heterogeneous photocatalytic reaction should be a first-order reaction if only one type of species adsorbed on the surface.[40] However, the experiment data often deviate from a first-order reaction with respect to the concentration of adsorbed species.[39] This is because more than one type of adsorbed species may exist on the surface with different atomic configurations and adsorption strength. Previous PEC studies of photocatalytic degradation of oxalic acid by the single layered anatase DF photoanode revealed that the overall photocurrent decay profiles can be well-fitted into a two exponential expression.[9, 12] The results also confirm that the surface adsorbed complexes can be simultaneously oxidized via two different first-order kinetic processes: one is fast (denoted as *f*) and another is slow (denoted as *s*). The two distinct kinetic decay processes represent two different types of adsorbed sites. The slow kinetic process can be attributed to the photocatalytic degradation of the intermediately and weakly bound surface complex, while the fast kinetic process is closely related to the strongly adsorbed surface complex.[9, 12, 31] The overall photocurrent decay profiles can be expressed as:

$$I_{ph} = I_{blank} + I^0_{phs} e^{-k_s t} + I^0_{phf} e^{-k_f t} \quad (2)$$

where I_{blank} is the steady photocurrent corresponding to the photocatalytic oxidation of water under UV illuminations. I^0_{phs} and I^0_{phf} present the initial photocurrent generated from slow and fast photocatalytic oxidations, respectively. The values of the initial photocurrents are proportional to the initial surface coverage of the corresponding species, which are determined by the concentrations of oxalic acid in the pre-adsorption solutions. k_s and k_f are the instantaneous intrinsic rate constants

of the fast and slow kinetic processes, respectively, which are strongly related to the adsorption energies of analytes.

The net charge (Q) generated from the photocatalytic oxidation of the adsorbed oxalic acid can therefore be determined by the following equation:

$$Q = \int (I_{ph} - I_{blank})dt = \int (I^0_{phs} e^{-k_s t} + I^0_{phf} e^{-k_f t})dt \quad (3a)$$

$$Q = Q_s + Q_f \quad (3b)$$

where Q_s and Q_f represent the charges generated from the slow and fast kinetic processes, respectively.

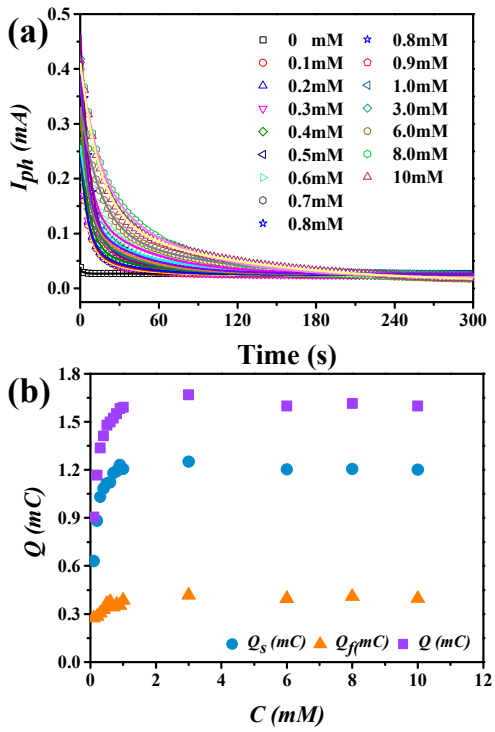

Fig. 3 (a) The photocurrent decay curves from photocatalytic degradation of adsorbed oxalic acid on the DL photoanode with different pre-adsorption concentrations at pH 4.0 and the curve-fitting data; (b) The adsorption isotherms of the fast and slow kinetic components and total for oxalic acid: (■) total adsorption (Q), (●) and (▲) adsorbed amounts responsible for the slow (Q_s) and fast (Q_f) kinetic process.

In this study, the pre-adsorption of oxalic acid occurs in a 0.1 M $NaNO_3$ solution with the concentration of oxalic acid (C) ranged from 0.1 mM to 10.0 mM at pH 4.0. Fig. 3a shows the photocurrent decay curves from the PEC degradation of the pre-adsorbed oxalic acid on {001} facts dominated DL photoanode. Based on the curve-fitting results using the Eq. (2), the values of I^0_{phs} , I^0_{phf}, k_s, and k_f, for the PEC degradation of adsorbed oxalic acid on the DL photoanode were calculated (see Tables S1, ESI†). The Q_s and Q_f were then calculated according to Eq (4) (details can be found from Eq. S1, ESI†):

$$Q_s = \frac{I^0_{phs}}{k_s},\ Q_f = \frac{I^0_{phf}}{k_f} \quad (4)$$

The calculated values for Q_s, Q_f, and Q based on Eqs. (3) and (4) are given in Table S2. The profiles of Q_s, Q_f, and Q with C are illustrated in Fig. 3b. It can be seen that the main contribution to Q is from Q_s, while the $Q_s - C$ profile shows a similar trend as that of the $Q - C$. So, the intermediately and weakly bound surface complexes account for a large portion of the total pre-adsorbed oxalic acid species. On the other hand, the relatively small Q_f values indicate that the quantity of strongly bound oxalic acid surface complexes is much less than the intermediate and weakly bound surface complexes.

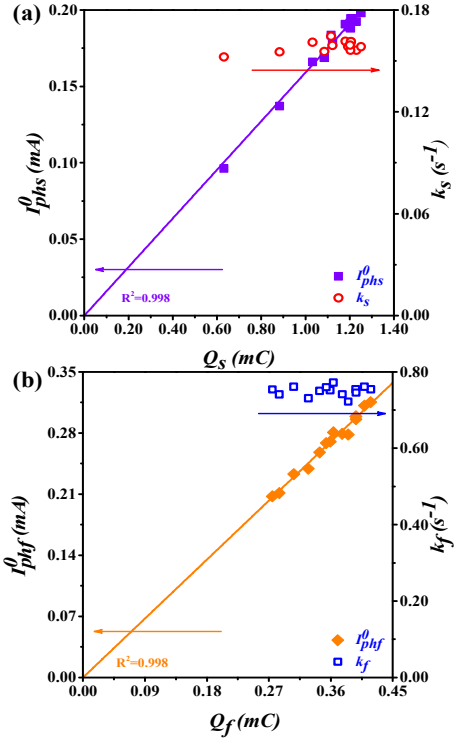

Fig. 4 (a) The plots of I^0_{phs} and k_s versus Q_s for the slow kinetic process: (o) first–order constant (k_s), (■) initial reaction rate (I^0_{phs}); (b) The plots of I^0_{phf} and k_f versus Q_f for the fast kinetic process: (□) first–order constant (k_f), (♦) initial reaction rate (I^0_{phf}).

Plots of I^0_{phs} and k_s versus Q_s for the slow kinetic species are shown in Fig 4a. It can be seen that the I^0_{phs} associated with the slow oxidation process are linearly correlated to the net transferred charge Q_s, which is determined by the concentration of oxalic acid. The average value of k_s is 0.16 s^{-1}, with small variations (±0.01 s^{-1}) over the oxalic acid concentration range investigated. Such small deviations suggest that the k_s values are independent of the concentration of oxalic acid. The plots shown in Fig 4b reflect the change of I^0_{phf} and k_f with the net transferred charge Q_f during the fast kinetic process. Similar $I^0_{phf} - Q_f$ and $k_f - Q_f$ relationships are found. The average value of k_f is 0.75 s^{-1} with deviations less than 0.02 s^{-1} over the entire range of considered oxalic acid concentrations. These results are qualitatively agreed with those previously obtained data from the DF photoanode (see Fig. S7, ESI†).[9] This means that the adsorption behaviors of oxalic acid on {001} faceted anatase TiO_2 surfaces is similar to that of {101} faceted anatase TiO_2 surfaces. The above results suggest that the average values of k_s and k_f obtained from the DL photoanode with exposed

{001} facets are 47% and 23% larger than those obtained from the DF photoanode with exposed {101} facets, respectively. The larger rate constants for both the slow and fast kinetic processes obtained from the DL photoanode confirm that the reactivity of the anatase TiO_2 (001) surface is higher, as predicted by theoretical studies.[21]

It should be noted that the presence of the fast and slow kinetic processes suggest the existence of two types of active sites at the surface of the photoanodes,[9, 12] which could be due to the presence of defects and/or different crystal facets, considering the DL photoanode consists of the mixed {001} and {101} facets.

Conclusions

In summary, a DL photoanode with a {101} facet dominated dense bottom layer and an {001} facet nominated top layer has been purposely fabricated and successfully used for PEC determination of the adsorption constant and the instantaneous intrinsic rate constants of photocatalytic degradation of the adsorbed oxalic acid. The results indicate that the adsorption constant of oxalic acid at a {001} facet nominated surface is 30% larger than that of a {101} facet nominated surface. The results also indicate that the average rate constant values of the slow and fast kinetic processes obtained from a photoanode with exposed {001} facet nominated surface are 47% and 23% larger than those obtained from a photoanode with exposed {101} facet nominated surface. This confirms that an anatase TiO_2 photocatalyst with {001} facets dominated surface possess higher photocatalytic activity than a photocatalysts with a {001} facets dominated surface. The method demonstrated in this work could be used to quantitatively investigate the photocatalytic degradation of other organic compounds.

Acknowledgements

We thank the Australian Research Council (ARC) and the Natural Science Foundation of China (Grant No. 51372248) for funding.

Notes and references

[a] *Centre for Clean Environment and Energy, and Griffith School of Environment, Gold Coast Campus, Griffith university, QLD 4222, Australia.; Fax: +61 1-55528067; Tel: +61 1-55528261*

[b] *Centre for Environmental and Energy Nanomaterials, Institute of Solid State Physics, Chinese Academy of Sciences, Hefei 230031, China*

E-mail: yun.wang@griffith.edu.au, h.zhao@griffith.edu.au

Electronic Supplementary Information (ESI) available: [details of any supplementary information available should be included here]. See DOI: 10.1039/c000000x/

Reference

1. X. Chen and S. S. Mao, *Chem. Rev.*, 2007, **107**, 2891-2959.
2. A. Fujishima and X. T. Zhang, *C. R. Chim.*, 2006, **9**, 750-760.
3. L. M. Peter, *Chem. Rev.*, 1990, **90**, 753-769.
4. A. Fujishima, X. T. Zhang and D. A. Tryk, *Surf. Sci. Rep.*, 2008, **63**, 515-582.
5. A. L. Linsebigler, G. Q. Lu and J. T. Yates, *Chem. Rev.*, 1995, **95**, 735-758.
6. M. A. Henderson, *Surf. Sci. Rep.*, 2011, **66**, 185-297.
7. A. G. Thomas and K. L. Syres, *Chem. Soc. Rev.*, 2012, **41**, 4207-4217.
8. D. L. Jiang, S. Q. Zhang and H. J. Zhao, *Environ. Sci. Technol.*, 2007, **41**, 303-308.
9. D. L. Jiang, H. J. Zhao, S. Q. Zhang and R. John, *J. Catal.*, 2004, **223**, 212-220.
10. D. L. Jiang, H. J. Zhao, S. Q. Zhang and R. John, *J Photoch Photobio A*, 2006, **177**, 253-260.
11. H. Zhao, D. Jiang, S. Zhang, K. Catterall and R. John, *Anal.Chem*, 2003, **76**, 155-160.
12. H. Zhao, D. Jiang, S. Zhang and W. Wen, *J. Catal.*, 2007, **250**, 102-109.
13. D. Jiang, H. Zhao, S. Zhang and R. John, *J.Phys.Chem.B*, 2003, **107**, 12774-12780.
14. D. Jiang, H. Zhao, Z. Jia, J. Cao and R. John, *J. Photochem. Photobiol. A: Chem.*, 2001, **144**, 197-204.
15. H. G. Yang, C. H. Sun, S. Z. Qiao, J. Zou, G. Liu, S. C. Smith, H. M. Cheng and G. Q. Lu, *Nature*, 2008, **453**, 638-641.
16. O. Dulub, M. Batzill, S. Solovev, E. Loginova, A. Alchagirov, T. E. Madey and U. Diebold, *Science*, 2007, **317**, 1052-1056.
17. N. Shibata, A. Goto, S. Y. Choi, T. Mizoguchi, S. D. Findlay, T. Yamamoto and Y. Ikuhara, *Science*, 2008, **322**, 570-573.
18. S. Wendt, P. T. Sprunger, E. Lira, G. K. H. Madsen, Z. S. Li, J. O. Hansen, J. Matthiesen, A. Blekinge-Rasmussen, E. Laegsgaard, B. Hammer and F. Besenbacher, *Science*, 2008, **320**, 1755-1759.
19. Y. Wang, T. Sun, X. L. Liu, H. M. Zhang, P. R. Liu, H. G. Yang, X. D. Yao and H. J. Zhao, *Phys Rev B*, 2014, **90**.
20. Z. C. Lai, F. Peng, Y. Wang, H. J. Wang, H. Yu, P. R. Liu and H. J. Zhao, *J. Mater. Chem.*, 2012, **22**, 23906-23912.
21. X. Q. Gong and A. Selloni, *J. Phys. Chem. B*, 2005, **109**, 19560-19562.
22. A. Vittadini, A. Selloni, F. P. Rotzinger and M. Gratzel, *Phys. Rev. Lett.*, 1998, **81**, 2954-2957.
23. S. Selcuk and A. Selloni, *J. Phys. Chem. C*, 2013, **117**, 6358-6362.
24. B. Liu and E. S. Aydil, *Chem. Commun.*, 2011, **47**, 9507-9509.
25. H. M. Zhang, Y. Wang, P. R. Liu, Y. H. Han, X. D. Yao, J. Zou, H. M. Cheng and H. J. Zhao, *ACS Appl. Mater. Interfaces*, 2011, **3**, 2472-2478.
26. P. R. Liu, Y. Wang, H. M. Zhang, T. C. An, H. G. Yang, Z. Y. Tang, W. P. Cai and H. J. Zhao, *Small*, 2012, **8**, 3664-3673.
27. D. L. Jiang, H. J. Zhao, S. Q. Zhang, R. John and G. D. Will, *J Photoch Photobio A*, 2003, **156**, 201-206.
28. D. Jiang, S. Zhang and H. Zhao, *Environ. Sci. Technol*, 2006, **41**, 303-308.
29. S. Zhang, H. Zhao, D. Jiang and R. John, *Anal.Chimica.Acta*, 2004, **514**, 89-97.
30. M. K. Nazeeruddin, A. Kay, I. Rodicio, R. Humphrybaker, E. Muller, P. Liska, N. Vlachopoulos and M. Gratzel, *J. Am. Chem. Soc.*, 1993, **115**, 6382-6390.
31. Y. Wang, H. M. Zhang, Y. H. Han, P. R. Liu, X. D. Yao and H. J. Zhao, *Chem. Comm.*, 2011, **47**, 2829-2831.
32. T. Berger, A. Rodes and R. Gomez, *Phys. Chem. Chem. Phys.*, 2010, **12**, 10503-10511.
33. J. Kulas, I. Rousar, J. Krysa and J. Jirkovsky, *J. Appl. Electrochem.*, 1998, **28**, 843-853.
34. H. G. Yang, G. Liu, S. Z. Qiao, C. H. Sun, Y. G. Jin, S. C. Smith, J. Zou, H. M. Cheng and G. Q. Lu, *J. Am. Chem. Soc.*, 2009, **131**, 4078-4083.
35. X. Wang, G. Liu, L. Wang, J. Pan, G. Q. Lu and H.-M. Cheng, *J.Mater.Chem*, 2011, **21**, 869-873.
36. P. J. Cameron, L. M. Peter and S. Hore, *J. Phys. Chem. B*, 2005, **109**, 930-936.
37. U. Diebold, *Surf. Sci. Rep.*, 2003, **48**, 53-229.
38. I. Ivanova, J. Schneider, H. Gutzmann, J. O. Kliemann, F. Gartner, T. Klassen, D. Bahnemann and C. B. Mendive, *Catal. Today*, 2013, **209**, 84-90.

39. C. B. Mendive, T. Bredow, A. Feldhoff, M. A. Blesa and D. Bahnemann, *Phys. Chem. Chem. Phys.*, 2009, **11**, 1794-1808.
40. S. R. Morrison, *Electrochemistry at Semiconductor and Oxidized Metal Electrodes*, Springer, Plenum, New York, 1980.